A fast and effective method for modelling and optimizing district heating systems in the Modelica language

Haoran Li [a,*], Juan Hou [a], Natasa Nord [a]

[a] *Department of Energy and Process Technology, Norwegian University of Science and Technology, Kolbjørn Hejes vei 1 B, Trondheim 7491, Norway*
corresponding. haoranli@ntnu.no

Abstract

A district heating system is a centralized energy system that supplies heat to end users such as buildings and industrial facilities. This centralized system may have multiple heat sources, a complex distribution network, and a large number of end users. Moreover, the heat distribution and utilization processes entail tumultuous thermal dynamics. Therefore, modelling and optimizing such a system generally demands arduous labour and necessitates powerful computing resources. To overcome these difficulties, this study introduced a fast and effective method for modelling and optimizing district heating systems using the Modelica language. Firstly, a simplified district heating system model was developed. This simplified model lumped all the end-users into a single thermal pinot with critical physical constraints. Meanwhile, the distribution network was simplified into two pipelines: supply and return. In addition, a one-dimensional discrete model was used to describe the behaviours of water tank thermal energy storage. Other essential components, like central and distributed heat sources, were modelled using basic mass and energy balance equations. Afterwards, two optimization frameworks were formulated, which incorporated the developed system model: a long-term optimal operation framework aimed at a yearly level open-loop optimization with a two-hour resolution, and a model predictive control framework aimed at a daily level close-loop optimization with a one-hour resolution. The proposed method was tested numerically on a university campus district heating system in Norway on a personal computer. Model validation showed that the proposed modelling approach could capture the key characteristics of the studied system. Optimization results demonstrated the effectiveness of the proposed optimization frameworks both for the long-term and short-term optimization.

1. Introduction

Buildings consume a considerable amount of energy and contribute significantly to global warming. In the European Union (EU), buildings account for roughly 40% of overall energy consumption and 36% of greenhouse gas emissions (*In focus: Energy efficiency in buildings*). As important parts of building energy systems, space heating (SH) and domestic hot water (DHW) systems play a crucial role in the energy usage of buildings. For example, in the EU's residential sector, SH and DHW account for over 80% of energy use (*Heating and cooling- European Commission*). District heating (DH) systems are a cost-effective and environmentally responsible approach to meeting buildings' heat demand (Li & Nord, 2018). Because of these advantages, DH systems are competitive with alternative heating methods, particularly in urban areas with high heat demand. In Europe, around 4,000 DH systems are currently operational (Sayegh et al., 2017), with DH systems accounting for up to 60% of the national heat market share in some countries (Åberg et al., 2020; Connolly et al., 2014; Werner, 2017). Despite these advantages of DH systems, no viable open-source platform focusing on the optimal design of DH systems and their control systems exists.

Modelica is a promising open-source language for modelling energy systems with numerous libraries. Recently, the Modelica language is further promoted by several large-scale international projects. Among these projects, IBPSA Project 1 has built the basis of the next generation computing tools for district energy and control systems (*IBPSA Project 1*, Jan 2021). However, the current Modelica based platforms show inadequate performance on computing DH systems and their control systems, especially for the cases with large scale and complex systems. Furthermore, modelling such a system is typically time-consuming, which adds to the difficulty of modelling and optimizing DH systems. To overcome these challenges, this article proposes a fast and effective method for modelling and

optimizing DH systems using the Modelica language. This article reports the research outcomes from several recent publications (Hou et al., 2019; Hou, Li, & Nord, 2022; Hou, Li, Nord, et al., 2022; Li et al., 2021; Li, Hou, Hong, et al., 2022; Li, Hou, Tian, et al., 2022; Li & Nord, 2019).

2. Modelling DH systems in Modelica

As illustrated in Figure 1, the proposed DH system model included a building, distribution pipeline, water tank thermal energy storage (WTTES), main substation, and distributed heat source (DHS) component. Due to the object-oriented nature of the Modelica language, it is possible to model a complete DH system by integrating these components. The detailed modelling work for these components is presented in Sections 2.1 to 2.4.

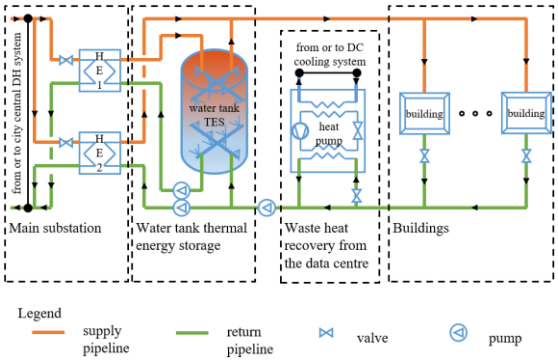

Figure 1: Configuration of the studied DH system.

2.1. Main substation and distributed heat source model

The energy balance equation was used to model the main substation and distributed heat source, as shown in Equations (1) to (4). The main substation has two heat exchangers, heat exchanger 1 and heat exchanger 2, working as charging and boosting heat sources, respectively. The distributed heat source may be solar thermal plants and waste heat recovery facilities.

$$\dot{Q}(t) = \dot{Q}_{HE1} + \dot{Q}_{HE2} \tag{1}$$

$$\dot{Q}_{HE1} = c \cdot \dot{m}_{HE1} \cdot (T_{HE1,sup} - T_{HE1,ret}) \tag{2}$$

$$\dot{Q}_{HE2} = c \cdot \dot{m}_{HE2} \cdot (T_{HE2,sup} - T_{HE2,ret}) \tag{3}$$

$$\dot{Q}_{DHS} = c \cdot \dot{m}_{DHS} \cdot (T_{DHS,sup} - T_{DHS,ret}) \tag{4}$$

where $\dot{m}_{HE1}$, $\dot{m}_{HE2}$, and $\dot{m}_{DHS}$ are the water flow rate of the heat exchanger 1, heat exchanger 2, and distributed heat source, respectively. $\dot{Q}_{HE1}$, $\dot{Q}_{HE2}$, and $\dot{Q}_{DHS}$ are the heat flow rate of the heat exchanger 1, heat exchanger 2, and distributed heat source, respectively. $T_{HE1,sup}$, $T_{HE2,sup}$, and $T_{DHS,sup}$ are the supply water temperature of the heat exchanger 1, heat exchanger 2, and distributed heat source, respectively. $T_{HE1,ret}$, $T_{HE2,ret}$, and $T_{DHS,ret}$ are the return water temperature of the heat exchanger 1, heat exchanger 2, and distributed heat source, respectively. c is the specific heat capacity of water.

2.2. Buildings model

The overall performance of all the buildings in a DH system was represented by a single-equivalent building model to improve computing efficiency. Following this simplification, the thermal behaviour of all the buildings was described using Equation (5). Inequality constraints for the water temperature and flow rate variables were given by Equations (6), (7), and (8).

$$\dot{Q}_{Bui} = c \cdot \dot{m}_{Bui} \cdot (T_{sup} - T_{ret}) \tag{5}$$

$$\Delta T_{Bui,L} \le \Delta T_{Bui} = T_{sup} - T_{ret} \le \Delta T_{Bui,U} \tag{6}$$

$$T_{sup,L} \le T_{sup} \le T_{sup,U} \tag{7}$$

$$\dot{m}_{Bui,L} \le \dot{m}_{Bui} \le \dot{m}_{Bui,U} \tag{8}$$

where $\dot{Q}_{Bui}$ is the total building heat demand, including the heat demand for SH and DHW systems as shown in Equation (9). $\dot{Q}_{SH}$ can be further divided into the demand for the radiator heating system $\dot{Q}_{rad}$ and the demand for the ventilation system $\dot{Q}_{ven}$, as described in Equation (10). $\dot{m}_{Bui}$ and ΔT_{Bui} are the mass flow rate and temperature difference for water at the primary side of the building substation, respectively. T_{sup} and T_{ret} are the supply and return temperature of water at the primary side of the building substation, respectively. $\Delta T_{Bui,L}$, $T_{sup,L}$, and $\dot{m}_{Bui,L}$ are the lower bounds for ΔT_{Bui}, T_{sup}, and $\dot{m}_{Bui}$, respectively. $\Delta T_{Bui,U}$, $T_{sup,U}$, and $\dot{m}_{Bui,U}$ are the upper bounds for ΔT_{Bui}, T_{sup}, and $\dot{m}_{Bui}$, respectively.

$$\dot{Q}_{Bui} = \dot{Q}_{SH} + \dot{Q}_{DHW} \tag{9}$$

$$\dot{Q}_{SH} = \dot{Q}_{rad} + \dot{Q}_{ven} \tag{10}$$

Buildings' dynamics were described using a simplified-lumped-capacity model generated from resistance-capacitance networks analogous to electric circuits, as stated in Equations (11), (12), and (13).

$$C_{env} \cdot \frac{dT_{env}}{dt} = \frac{T_{ia} - T_{env}}{R_{i,e}} + \frac{T_{oa} - T_{env}}{R_{o,e}} \tag{11}$$

$$C_{ia} \cdot \frac{dT_{ia}}{dt} = \frac{T_{ma} - T_{ia}}{R_{i,m}} + \frac{T_{env} - T_{ia}}{R_{i,e}} + \frac{T_{oa} - T_{ia}}{R_{win}} + \frac{T_{oa} - T_{ia}}{R_{ven}} + \dot{Q}_{rad} + \dot{Q}_{ven} + \dot{Q}_{in} \quad (12)$$

$$C_{ma} \cdot \frac{dT_{ma}}{dt} = \frac{T_{ia} - T_{ma}}{R_{i,m}} \quad (13)$$

where C and R are the heat capacitance and resistance, and T refers to the temperature. Building envelopes (including exterior walls and roofs), indoor air, outdoor air, internal thermal mass, window, and ventilation (including infiltration and mechanical ventilation) are denoted by the subscripts ven, ia, oa, ma, win, and ven, respectively. $R_{i,e}$ represents the heat resistance between indoor air and building envelopes, $R_{o,e}$ represents the heat resistance between outdoor air and building envelopes, and $R_{i,m}$ represents the heat resistance between indoor air and interior thermal mass. $\dot{Q}_{in}$ is the internal heat gain.

As described in Equation (14), the lower bound of the supply temperature should be high enough for the SH and DHW systems to maintain a comfortable indoor temperature while avoiding hygiene problems. Equation (15) defined the lower bound of the supply temperature for the SH system (He et al., 2009), whereas Equation (16) determined the lower bound for the DHW system, which is required by European standard CEN/TR16355 ("CEN/TR16355 Recommendations for prevention of Legionella growth in installations inside buildings conveying water for human consumption," 2012).

$$T_{sup,L} = max(T_{sup,SH,L}, T_{sup,DHW,L}) \quad (14)$$

$$T_{sup,SH,L} = T_{ia} + 0.5 \cdot (T_{sup,SH,des} + T_{ret,SH,des} - 2 \cdot T_{ia,des}) \cdot (\frac{T_{ia,des} - T_{oa}}{T_{ia,des} - T_{oa,des}})^{1/b} + 0.5 \cdot (T_{sup,SH,des} - T_{ret,SH,des}) \cdot (\frac{T_{ia,des} - T_{oa}}{T_{ia,des} - T_{oa,des}}) \quad (15)$$

$$T_{sup,DHW,L} = 60℃ \quad (16)$$

where $T_{sup,SH,L}$ and $T_{sup,DHW,L}$ are the lower bounds for the SH and DHW system's supply temperatures, respectively. T_{ia} and T_{oa} are the indoor and outdoor air temperatures, respectively. $T_{sup,SH}$ and $T_{ret,SH}$ are the supply and return temperatures for the SH system, respectively. b is a parameter defining the radiator's characteristic. des is a subscript that refers to the design conditions.

The lower bound of the water mass flow rate $\dot{m}_{Bui,L}$ was zero, while the upper bound $\dot{m}_{Bui,U}$ was constrained by the distribution system's capacity. In addition, the lower bound of the water temperature difference $\Delta T_{Bui,L}$ was zero, and the upper bound of the water temperature difference $\Delta T_{Bui,U}$ was obtained from linear regression Equation (17).

$$\Delta T_{Bui,U} = a_0 + a_1 \cdot T_{sup} \quad (17)$$

where a_0 and a_1 are parameters.

2.3. Distribution pipeline model

Equations (18), (19), and (20) were used to describe the heat loss from pipelines.

$$\dot{Q}_{loss,pip} = \dot{Q}_{loss,pip,sup} + \dot{Q}_{loss,pip,ret} \quad (18)$$

$$\dot{Q}_{loss,pip,sup} = L \cdot \pi \cdot d \cdot \frac{(R_g + R_i) \cdot \Delta T_{pip,sup} - R_c \cdot \Delta T_{pip,ret}}{(R_g + R_i)^2 - {R_c}^2} \quad (19)$$

$$\dot{Q}_{loss,pip,ret} = L \cdot \pi \cdot d \cdot \frac{(R_g + R_i) \cdot \Delta T_{pip,ret} - R_c \cdot \Delta T_{pip,sup}}{(R_g + R_i)^2 - {R_c}^2} \quad (20)$$

where $\dot{Q}_{loss,pip}$, $\dot{Q}_{loss,pip,sup}$, and $\dot{Q}_{loss,pip,ret}$ represent the overall heat loss from pipes, supply pipe heat loss, and return pipe heat loss, respectively. L refers to the route length for the pair of pipes. d is the outer pipe diameter. R_i, R_g, and R_c are the resistances for the insulation, ground, and coinciding, respectively, and they can be obtained by Equations (21), (22) and (23), respectively. $\Delta T_{pip,sup}$ and $\Delta T_{pip,ret}$ are the temperature differences for the supply and return pipes, respectively, and can be obtained using Equations (24) and (25).

$$R_i = \frac{d}{2 \cdot \lambda_i} \cdot ln\frac{D}{d} \quad (21)$$

$$R_g = \frac{d}{2 \cdot \lambda} \cdot ln\frac{4 \cdot h}{D} \quad (22)$$

$$R_c = \frac{d}{2 \cdot \lambda} \cdot ln(((\frac{2 \cdot h}{s})^2 + 1)^{0.5}) \quad (23)$$

$$\Delta T_{pip,sup} = T_{pip,sup} - T_{grou} \quad (24)$$

$$\Delta T_{pip,ret} = T_{pip,ret} - T_{grou} \quad (25)$$

where D is the outer insulation diameter, h is the distance between the pipe centres and the ground

surface, s is the distance between pipe centres, and λ and λ_i are the heat conductivity for the ground and insulation, and T_{grou} is the ground temperature.

2.4. Water tank thermal energy storage model

The dynamics of the water tank were described using a one-dimensional WTTES model (Powell & Edgar, 2013).

$$c \cdot \rho \cdot A_{XS} \cdot \frac{\partial T}{\partial t} = c \cdot (\dot{m}_{sou} - \dot{m}_{use}) \cdot \frac{\partial T}{\partial x} - U \cdot P \cdot (T(t,x) - T_{amb}) + \varepsilon \cdot A_{XS} \cdot \frac{\partial^2 T}{\partial x^2} \quad (26)$$

where T is the water temperature. x is the height of the tank. t is the time. ρ is the water density. A_{XS} and P are the cross-sectional area and perimeter of the tank, respectively. $\dot{m}_{sou}$ and $\dot{m}_{use}$ are the water mass flow rate of the heat source and user side, respectively. T_{amb} is the ambient temperature. U is the U-value of the tank wall. ε is a parameter representing the combined heat transfer effect of water through diffusion, conduction, and mixing due to turbulent flow.

By discretizing the tank into n nodes, spatial derivatives were approximated using numerical techniques. Equation (27) shows the ordinary differential equation for the ith node. Equations (28) and (29) were used to compute the heat loss and heat flow rate of the ith node, while Equations (30) and (31) were used to get the total heat loss and heat flow rate of the WTTES.

$$c \cdot \rho \cdot A_{XS} \cdot \Delta x \cdot \frac{dT_i}{dt} = c \cdot \dot{m}_{use} \cdot (T_{i-1} - T_i) + c \cdot \dot{m}_{sou} \cdot (T_{i+1} - T_i) - U \cdot P \cdot \Delta x \cdot (T_i - T_{amb}) + \frac{\varepsilon \cdot A_{XS}}{\Delta x} \cdot (T_{i+1} - 2 \cdot T_i + T_{i-1}) \quad (27)$$

$$\dot{q}_{loss,TES,i} = U \cdot P \cdot \Delta x \cdot (T_i - T_{amb}) \quad (28)$$

$$\dot{q}_{TES,i} = c \cdot \dot{m}_{sou} \cdot (T_{i+1} - T_i) \quad (29)$$

$$\dot{Q}_{loss,TES} = \sum_{i=1}^{n-1} \dot{q}_{loss,TES,i} \quad (30)$$

$$\dot{Q}_{TES} = \sum_{i=1}^{n-1} \dot{q}_{TES,i} \quad (31)$$

where Δx is the node length, and T_i is the water temperature of the ith node. $\dot{q}_{loss,TES,i}$ and $\dot{q}_{TES,i}$ are the heat loss and heat flow rate of the ith node, respectively.

3. Optimization frameworks in JModelica

Two optimization frameworks were formulated: a long-term optimal operation framework aimed at a yearly level open-loop optimization with a two-hour resolution, and a model predictive control (MPC) framework aimed at a daily level close-loop optimization with a one-hour resolution. These two optimization frameworks used the same objective function, minimizing heating costs while tracking the reference indoor temperature, as shown in Equation (32). In addition, these two optimization frameworks used the same system dynamic models and inequality constraints introduced in Section 2, as shown in Equations (33), (34), (35), and (36).

$$\int_{t_0}^{t_f} EP(t) \cdot \dot{Q}(t) dt + LP \cdot \dot{Q}_{pea} + W \cdot \int_{t_0}^{t_f} (T_{ia}(t) - T_{ia}^{ref}(t))^2 \cdot dt \quad (32)$$

subject to:

$$\dot{Q}(t) \leq \dot{Q}_{pea} \quad (33)$$

$$F(t, \boldsymbol{z}(t)) = 0 \quad (34)$$

$$F_0(t_0, \boldsymbol{z}(t_0)) = 0 \quad (35)$$

$$z_L \leq \boldsymbol{z}(t) \leq z_U \quad (36)$$

where $\dot{Q}(t)$ is the heat flow rate supplied from the central DH to the main substation. $\dot{Q}_{pea}$ and LP is the peak load and the peak load related heating price, respectively. $EP(t)$ is the heating price for the heat use related heating cost. $T_{ia}(t)$ and $T_{ia}^{ref}(t)$ are the simulated indoor temperature and its reference value at time t. $\boldsymbol{z} \in \mathbb{R}^{n_z}$ represents the time-dependent variables, which includes the manipulated variable $\boldsymbol{u} \in \mathbb{R}^{n_u}$ to be optimized, the differential variable $\boldsymbol{x} \in \mathbb{R}^{n_x}$, and the algebraic variable $\boldsymbol{y} \in \mathbb{R}^{n_y}$. Equation (34) defines the system dynamics and Equation (35) is the initial conditions of the system. $z_L \in [-\infty, \infty]^{n_z}$ and $z_U \in [-\infty, \infty]^{n_z}$ are the lower and upper bounds, respectively.

The long-term open-loop optimization framework is illustrated in Figure 2. This long-term optimization framework computes the optimal operation trajectory for a whole operating year. This framework was used for optimal design and operation in the research (Li, Hou, Hong, et al., 2022; Li, Hou, Tian, et al., 2022).

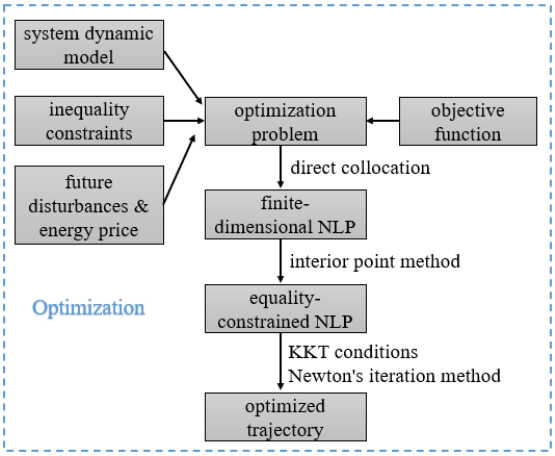

Figure 2: Long-term open-loop optimization framework for optimal design and operation.

The short-term close-loop optimization framework is illustrated in Figure 3. This short-term optimization framework computes the optimal operation trajectory within the prediction horizon (mostly from half to two days). This framework was used for MPC in a study presented in the results section 4.2.

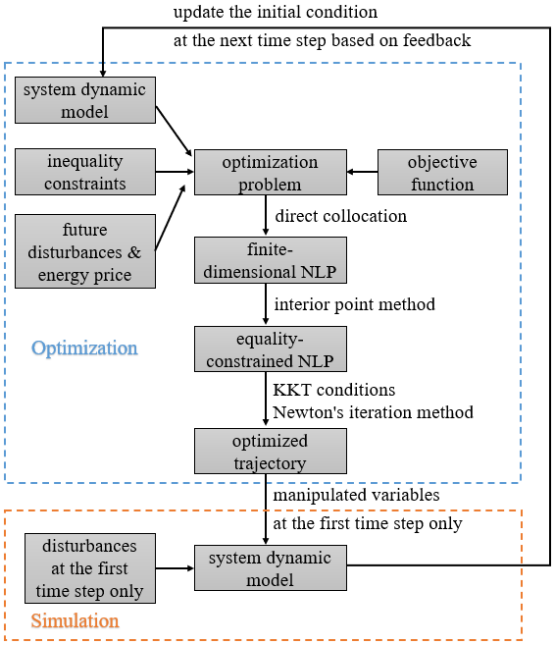

Figure 3: Short-term close-loop optimization framework for optimal control.

4. Case study

A campus DH system in Trondheim, Norway, was chosen as the case study. The campus DH system is a prosumer with a distributed heat source, as shown in Figure 4. The distributed heat source is the university data centre, which recovers the condensing waste heat from the data centre's cooling system. The campus DH system supplies heat for the university buildings with a total building area of 300,000 m^2. The main substation is used to connect the campus DH system with the city's central DH system. According to the measurements from June 2017 to May 2018, the total heat supply for the campus DH system was 32.8 GWh. About 80% of the heat supply came from the central DH system through the main substation. The other 20% came from the waste heat recovery from the data centre.

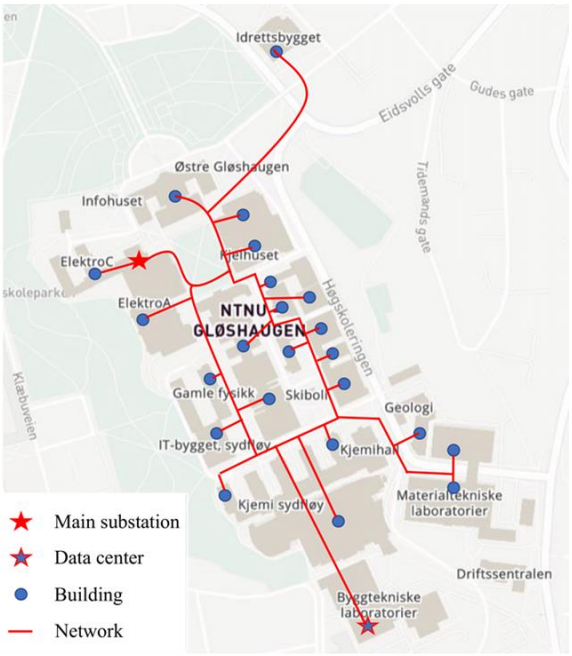

Figure 4: Campus district heating system.

5. Results

The developed DH system model presents high accuracy, and the results of model validation can be found in articles (Li, Hou, Hong, et al., 2022; Li, Hou, Tian, et al., 2022). This article only presents the key results on energy and economic performance of the long-term and short-term optimization frameworks.

5.1. Energy and economic performance of the long-term optimization framework

The long-term optimization framework tested the idea of introducing a WTTES into the campus DH system. Figure 5 and Figure 6 present the annual heat use and the yearly peak load for the scenario before and after introducing the WTTES, respectively. These two indicators quantified the heat supply from the central DH system to the heat prosumer through the main substation. It can be observed from Figure 5 that introducing the WTTES reduced the annual heat use from 26.2 GWh to 25.9 GWh, meaning a heat use saving of 1%. Compared to this less significant heat use saving, a more obvious peak load shaving was obtained as shown in Figure 6, the yearly peak load was shaved from 12.4 MW to 9.5 MW, a shaving of 24%.

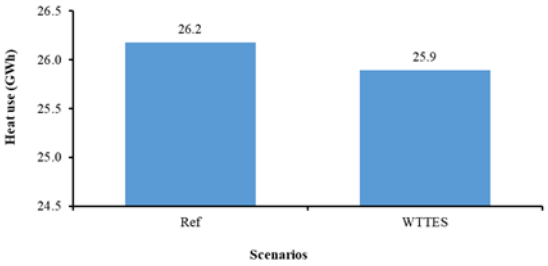

Figure 5: Annual heat use for the scenario before and after introducing WTTES.

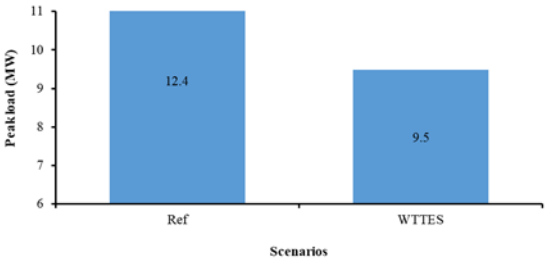

Figure 6: Yearly peak load for the scenario before and after introducing WTTES.

The resulting annual heating cost for the scenario before and after introducing WTTES is presented in Figure 7. Introducing WTTES cut the annual heating cost from 20.7 million NOK to 19.3 million NOK, which meant a cost saving of 7% was achieved.

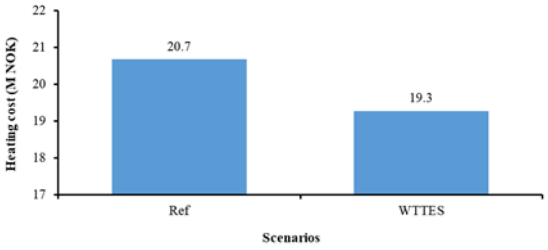

Figure 7: Annual heating cost for the scenario before and after introducing WTTES.

5.2. Energy and economic performance of the short-term optimization framework

The short-term optimization framework evaluated the potential of the MPC strategy. In this study, two scenarios, one MPC scenario and one rule-based control (RBC) scenario, were designed and compared. Figure 8 and Figure 9 present the heat use and peak load for the MPC and RBC scenario, respectively.

It can be observed from Figure 8 that the MPC scenario reduced the heat use from 5.12 GWh to 5.02 GWh in January, meaning a heat use saving of 2%. Meanwhile, in April the reduction was from 2.33 GWh to 2.25 GWh, a saving of 3%. Similar to the long-term optimization problem with less significant heat use saving, a more obvious peak load shaving was obtained as shown in Figure 9, the peak load was shaved from 11.6 MW to 10.9 MW in January, a shaving of 6%. In addition, the shaving was from 8.0 MW to 7.1 MW in April, a shaving of 11%.

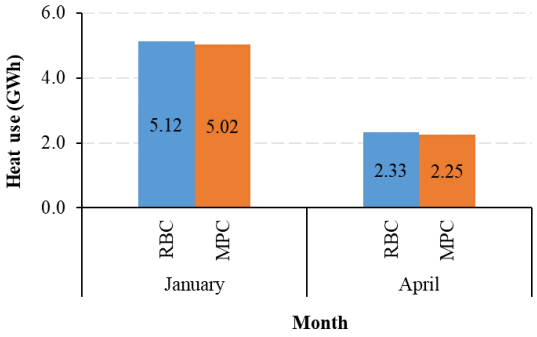

Figure 8: Heat use for the MPC and RBC scenario.

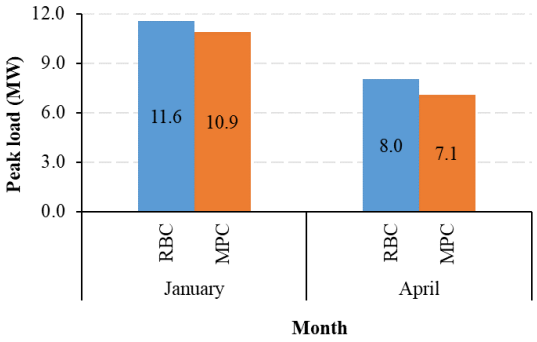

Figure 9: Peak load for the MPC and RBC scenario.

The resulting energy costs (including heating and electricity cost) for the MPC and RBC scenarios is presented in Figure 10. In Figure 10, the electricity cost included the spot price-related fee and surcharges, which had prices in NOK/kWh. The proposed MPC strategy cut the energy cost from 3.47 million NOK to 3.40 million NOK in January, which meant a cost saving of 2% was achieved. Meanwhile, the cutting was from 1.92 million NOK to 1.86 million NOK in April, a saving of 3%. These cost savings were subjected to the specified energy price models in this study. For other cases, the results may be different.

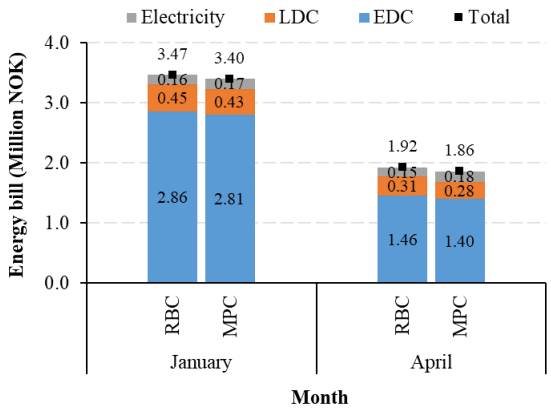

Figure 10: Heating cost for the MPC and RBC scenario.

6. Conclusion

This study presents a fast and effective method for modelling and optimizing DH systems using the Modelica language. A case study on a university campus DH system in Norway showed that the method was effective both for long-term optimal operation and short-term optimal control problems. For the studied case, the approach achieved energy cost saving by energy use reduction and peak demand shaving. It is worth noting that the achieved results may be subjected to specified energy price models, however, this study provided a generalized method to solve this type of research problem.

Acknowledgement

The authors gratefully acknowledge the support from the H2020 EU-funded project Climate Positive Circular Communities (grant agreement ID: 101036723), which aims at creating climate positive circular communities in Europe and increasing the building renovation rate in the continent.

References

Åberg, M., Fälting, L., Lingfors, D., Nilsson, A. M., & Forssell, A. (2020). Do ground source heat pumps challenge the dominant position of district heating in the Swedish heating market? *Journal of Cleaner Production*, *254*, 120070. https://doi.org/https://doi.org/10.1016/j.jclepro.2020.120070

CEN/TR16355 Recommendations for prevention of Legionella growth in installations inside buildings conveying water for human consumption. (2012). In.

Connolly, D., Lund, H., Mathiesen, B. V., Werner, S., Möller, B., Persson, U., Boermans, T., Trier, D., Østergaard, P. A., & Nielsen, S. (2014). Heat Roadmap Europe: Combining district heating with heat savings to decarbonise the EU energy system. *Energy Policy*, *65*, 475-489. https://doi.org/10.1016/j.enpol.2013.10.035

He, P., Sun, G., Wang, F., Wu, H., & Wu, X. (2009). *Heating engineering (in Chinese)*. China Architecture & Building Press.

Heating and cooling- European Commission. https://ec.europa.eu/energy/en/topics/energy-efficiency/heating-and-cooling

Hou, J., Li, H., & Nord, N. (2019). Optimal control of secondary side supply water temperature for substation in district heating systems. *E3S Web Conf.*, *111*, 06015. https://doi.org/10.1051/e3sconf/201911106015

Hou, J., Li, H., & Nord, N. (2022). Nonlinear model predictive control for the space heating system of a university building in Norway. *Energy*, *253*, 124157. https://doi.org/https://doi.org/10.1016/j.energy.2022.124157

Hou, J., Li, H., Nord, N., & Huang, G. (2022). Model predictive control under weather forecast uncertainty for HVAC systems in university buildings. *Energy and Buildings*, *257*, 111793. https://doi.org/https://doi.org/10.1016/j.enbuild.2021.111793

IBPSA Project 1. (Jan 2021). https://ibpsa.github.io/project1/index.html

In focus: Energy efficiency in buildings. (Jan 2021). https://ec.Europa.Eu/info/news/focus-energy-efficiency-buildings-2020-feb-17_en#:~:Text=collectively%2c%20buildings%20in%20the%20eu,%2c%20usage%2c%20renovation%20and%20demolition

Li, H., Hou, J., Hong, T., Ding, Y., & Nord, N. (2021). Energy, economic, and environmental analysis of integration of thermal energy storage into district heating systems using waste heat from data centres. *Energy*, *219*, 119582. https://doi.org/https://doi.org/10.1016/j.energy.2020.119582

Li, H., Hou, J., Hong, T., & Nord, N. (2022). Distinguish between the economic optimal and lowest distribution temperatures for heat-prosumer-based district heating systems with short-term thermal energy storage. *Energy*, *248*, 123601. https://doi.org/https://doi.org/10.1016/j.energy.2022.123601

Li, H., Hou, J., Tian, Z., Hong, T., Nord, N., & Rohde, D. (2022). Optimize heat prosumers' economic performance under current heating price models by using water tank thermal energy storage. *Energy*, *239*, 122103. https://doi.org/https://doi.org/10.1016/j.energy.2021.122103

Li, H., & Nord, N. (2018). Transition to the 4th generation district heating- possibilities, bottlenecks, and challenges. *Energy Procedia*, *149*, 483-498. https://doi.org/https://doi.org/10.1016/j.egypro.2018.08.213

Li, H., & Nord, N. (2019). Operation strategies to achieve low supply and return temperature in district heating system. *E3S Web Conf.*, *111*, 05022. https://doi.org/10.1051/e3sconf/201911105022

Powell, K. M., & Edgar, T. F. (2013). An adaptive-grid model for dynamic simulation of thermocline thermal energy storage

systems. *Energy Conversion and Management*, *76*, 865-873. https://doi.org/https://doi.org/10.1016/j.enconman.2013.08.043

Sayegh, M. A., Danielewicz, J., Nannou, T., Miniewicz, M., Jadwiszczak, P., Piekarska, K., & Jouhara, H. (2017). Trends of European research and development in district heating technologies. *Renewable and Sustainable Energy Reviews*, *68*, 1183-1192. https://doi.org/10.1016/j.rser.2016.02.023

Werner, S. (2017). International review of district heating and cooling [Review]. *Energy*, *137*, 617-631. https://doi.org/10.1016/j.energy.2017.04.045